Supplementary Figures

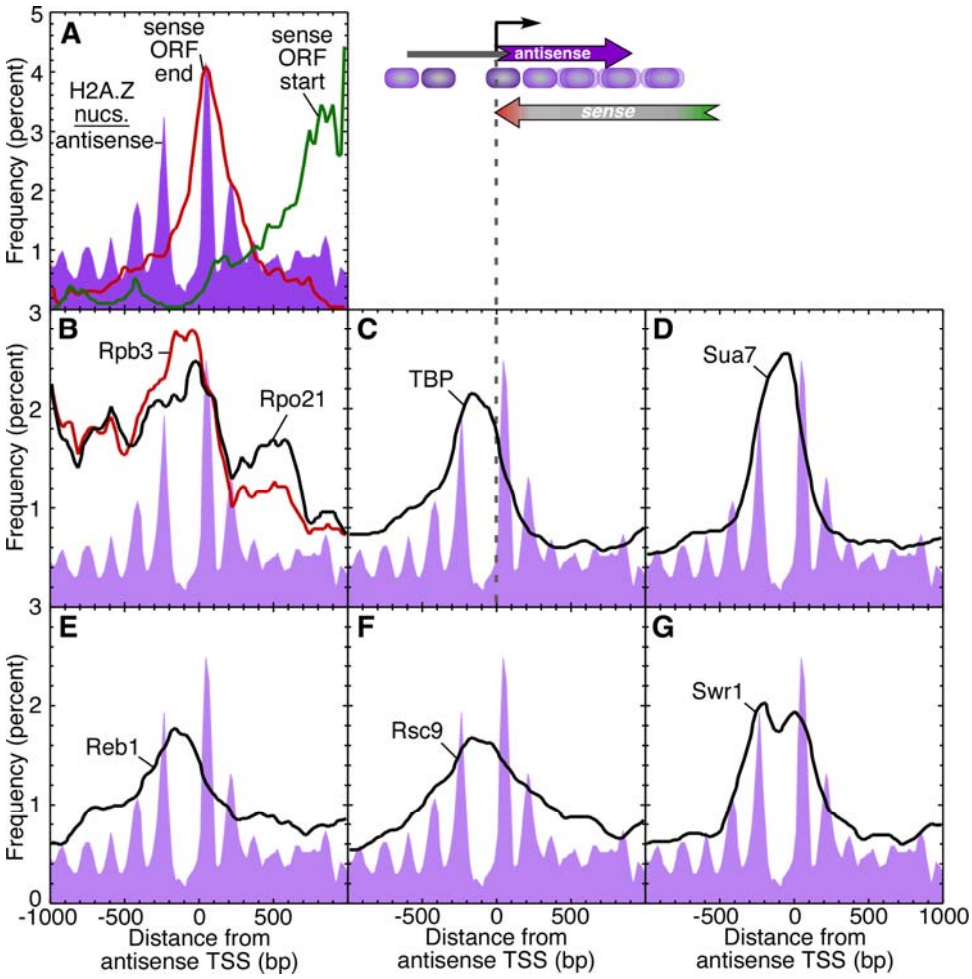

Figure S1. The distribution of the H2A.Z nucleosomes and the transcription machinery at sites of anti-sense transcription. The composite frequency distributions for the binding locations (peak calls from normalized signal) for representative components of the transcription machinery are shown for 194 sites of anti-sense transcription (Perocchi et al. 2007). These transcripts were selected to be anti-sense to an annotated gene but did not overlap with a sense gene. The graphs were generated as described in Figure 3 except that all identified ChIP-chip peaks were considered (i.e., no FDR cutoff was applied).

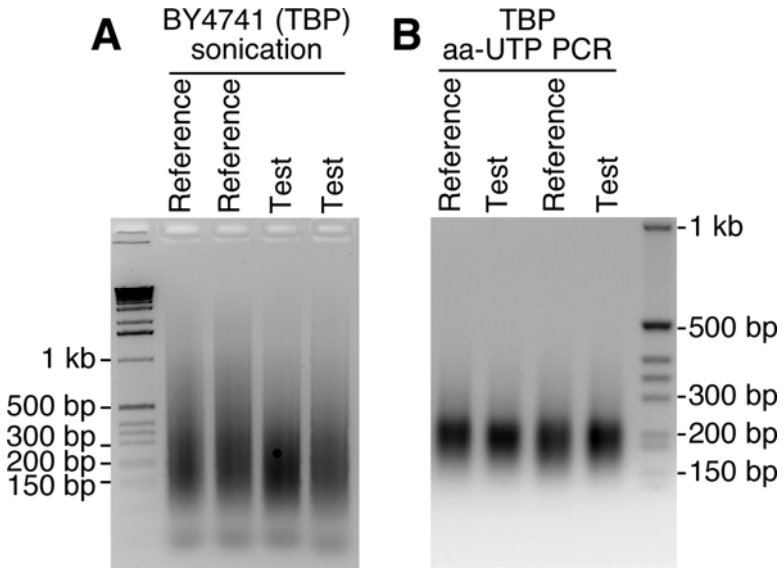

Figure S2. Sonicated input DNA and gel purified LM-PCR ChIP-enriched DNA size range. (**A**) Prior to ChIP, input chromatin was sonicated extensively to yield a median size of ~200 bp. (**B**) The LM-PCR amplified TBP ChIP eluate was gel-purified between 75 and 300bp in an effort to maximize the achievable resolving power on tiling microarrays.

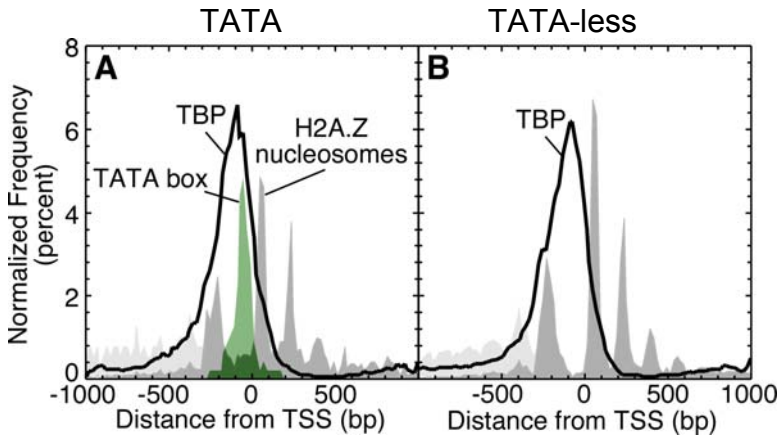

Figure S3. TBP binds the same consensus location relative to the TSS whether or not a TATA box is present. Genome-wide frequency distribution for H2A.Z nucleosomes determined by ChIP-seq (Albert et al. 2007) illustrates the nucleosomal architecture at the indicated set of promoters, shown in gray. The frequency distribution for conserved TATA consensus sites (Basehoar et al. 2004), is shown in green. The frequency distribution for TBP binding locations determined by ChIP-chip using Affymetrix high density tiling arrays is shown for TATA-containing promoters (**A**), and TATA-less promoters (**B**).

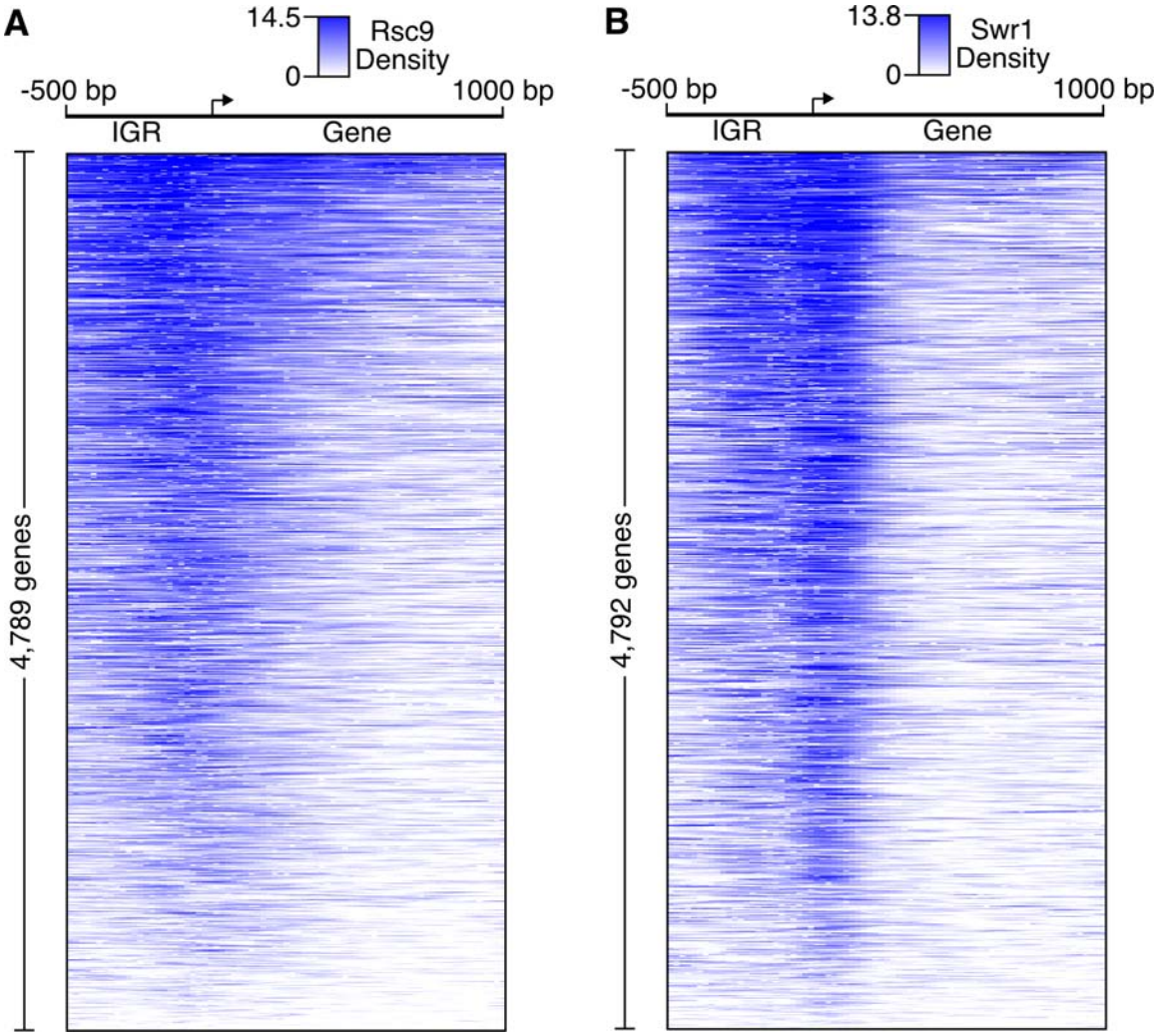

Figure S4. Cluster plot of Rsc9 and Swr1 density across individual genes. Normalized ChIP-chip signal was binned in 20 bp increments as an absolute distance from the TSS (-500 bp to 1000 bp). The normalized signal within each bin was averaged, and displayed using Treeview (Eisen et al. 1998). Individual genes are descending ordered from top to bottom by the average ChIP signal within a 1.5 kb window surrounding the transcription start site.

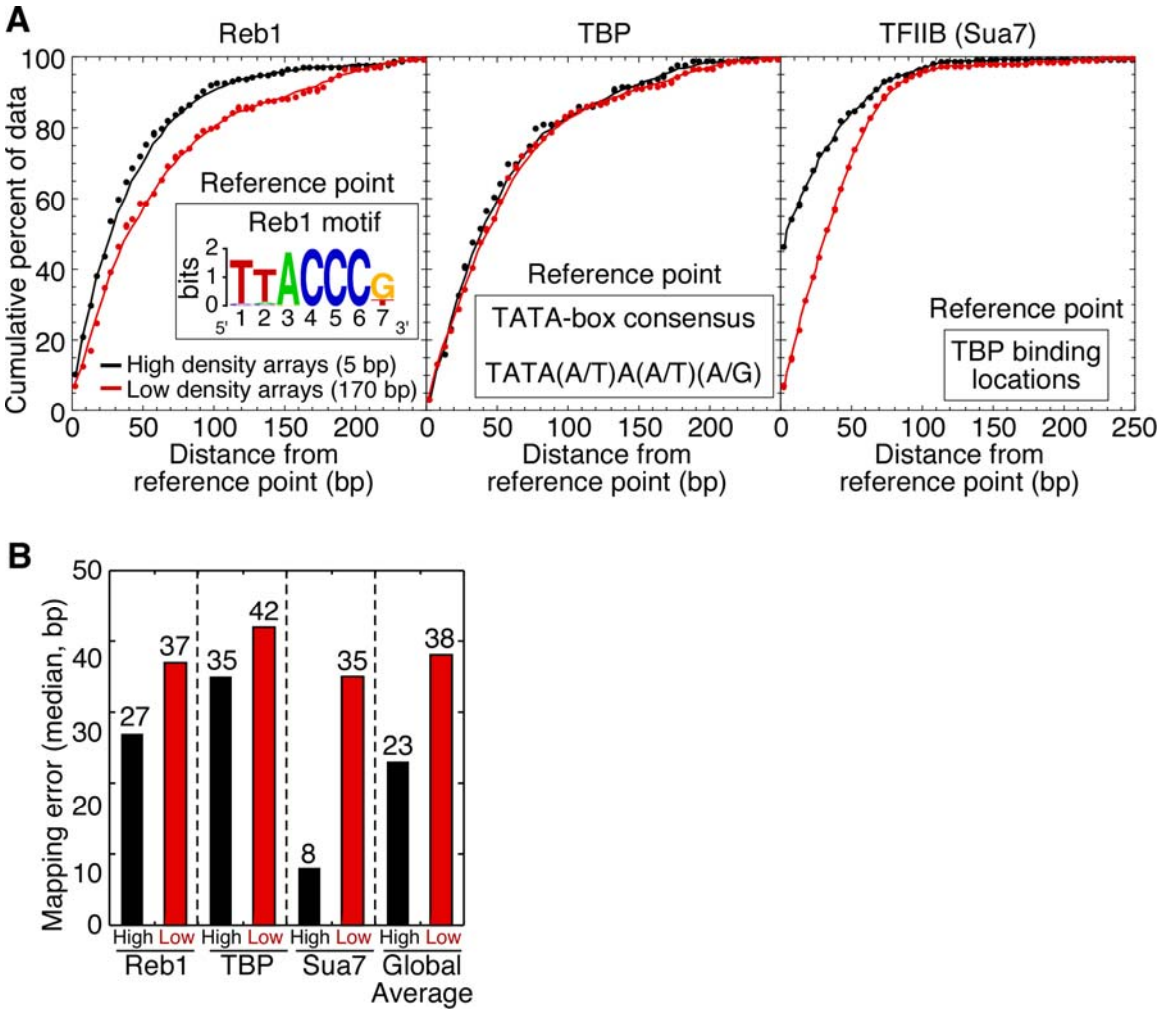

Figure S5. Low- and high-density tiling arrays yield similar mapping errors. The binding locations for Reb1, TBP, and Sua7 were experimentally determined by ChIP-chip on low- and high-density tiling arrays. (**A**) The distance from the cognate binding sites for Reb1 (i.e., the Reb1 motif shown in the plot), TBP (i.e., the TATA box motif shown in the plot), and Sua7 (i.e., the TBP binding location measured by high density arrays) is shown as a cumulative error plot. (**B**) The median mapping error for Reb1, TBP and Sua7 is displayed as a bar graph. "High" and "Low" denote high density Affymetrix arrays and low density arrays. Global average is the average of the individual mapping errors for Reb1, TBP, and Sua7.

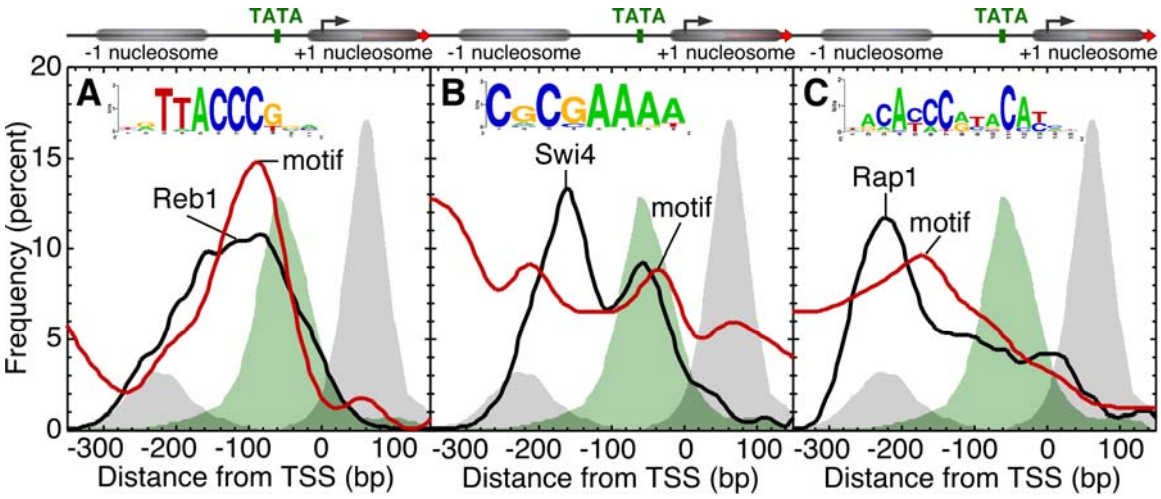

Figure S6. MEME was used to identify binding motifs for sequence-specific regulators (Bailey et al. 2006). A motif search in a +/-250bp window relative to the binding locations for determined by ChIP-chip was conducted. The frequency distributions for the Reb1 (**A**), Swi4 (**B**), and Rap1 (**C**) motifs are compared with that of the cognate transcription factor. The motifs identified agree with the corresponding published motifs (Harbison et al. 2004).

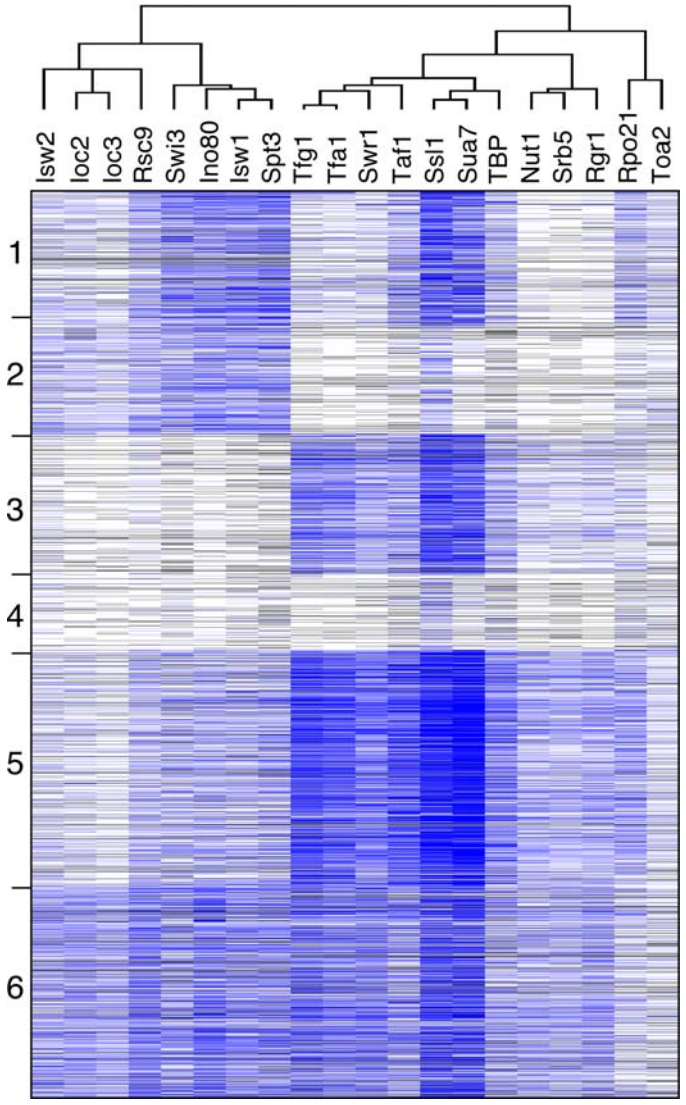

Figure S7. Cluster plot comparison of genomic locations of the transcription machinery. 5,866 genes were clustered by *K*-means into 6 visually nonredundant groups (all 5,866 genes are shown), and columns were hierarchically clustered with the resulting dendrogram shown above the plot. Each row represents an individual Pol II promoter region. Each column represents a ChIP-chip experiment for a given factor. The occupancy levels for each factor at a promoter were derived from low-density tiling arrays, where higher occupancy levels are shown by darker shades of blue a $\log_2$ scale. White denotes occupancy equal to or less than zero, and gray denotes no data present.

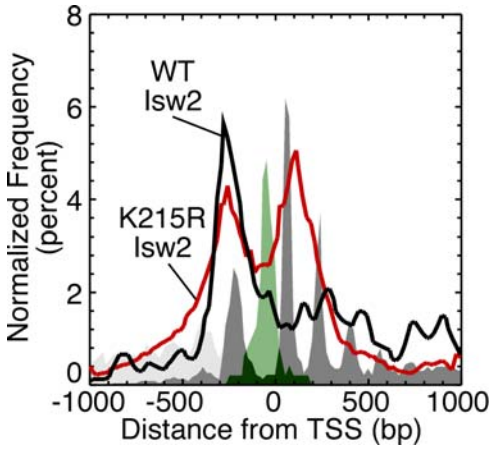

Figure S8. Composite frequency distribution for wild-type Isw2 and a catalytically inactive Isw2(K215R) mutant. Affymetrix high-density yeast tiling array cel files from a previously report (Whitehouse et al. 2007) were downloaded and analyzed using MAT software (Johnson et al. 2006). Peaks were called using a 5% FDR, and plotted as a composite frequency distribution. The local chromatin landscape of H2A.Z nucleosomes (Albert et al. 2007) is shown in gray, and the distribution of TATA boxes (Basehoar et al. 2004) shown in green, when present.

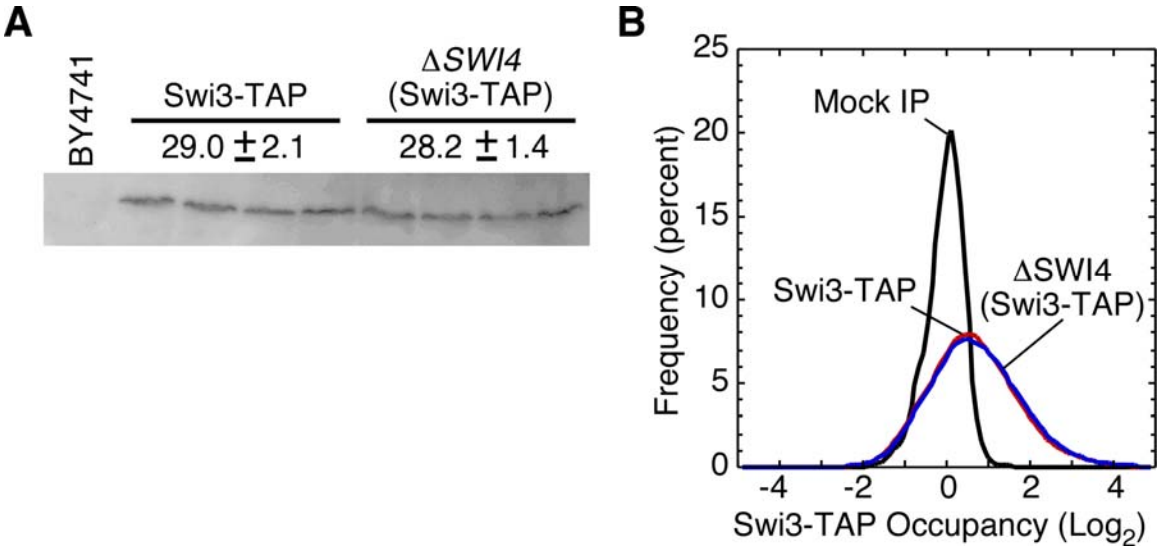

Figure S9. Loss of *SWI4* does not diminish Swi3-TAP expression or global distribution. (**A**) Shown is an immunoblot detection of the Swi3-TAP tag for the four biological replicates used in standard ChIP PCR for both wild-type and mutant strains. An untagged BY4741 strain was used as negative control. The average signal intensity and standard deviation for four independent replicates was quantified using Image J software, and the values are shown above the blot. (**B**) The global Swi3-TAP occupancy distributions in a wild-type and *swi4Δ* strain are shown.

Supplementary Tables

Table S1. Relationship of Pol II density patterns (Figure 4A) with published microarray data.

				Cluster[a] -log$_{10}$(*P*-value)		
Category	**Description**	**Protein/Characteristic**	**Percent Rank**	**1**	**2**	**3**
ChIP	Sequence-specific regulator	ABF1	Top 10%	10	5	0
ChIP	Sequence-specific regulator	ACE2	Top 10%	6	0	0
ChIP	Sequence-specific regulator	ADR1	Top 10%	10	1	1
ChIP	Sequence-specific regulator	ARG80	Top 10%	11	1	0
ChIP	Sequence-specific regulator	ARG81	Top 10%	13	1	0
ChIP	Sequence-specific regulator	ARO80	Top 10%	13	1	0
ChIP	Sequence-specific regulator	AZF1	Top 10%	8	0	0
ChIP	Sequence-specific regulator	BAS1	Top 10%	10	0	0
ChIP	Sequence-specific regulator	CAD1	Top 10%	9	0	0
ChIP	Sequence-specific regulator	CBF1	Top 10%	8	0	2
ChIP	Sequence-specific regulator	CHA4	Top 10%	12	0	1
ChIP	Sequence-specific regulator	CUP9	Top 10%	6	0	0
ChIP	Sequence-specific regulator	DAL81	Top 10%	5	3	0
ChIP	Sequence-specific regulator	DAL82	Top 10%	8	0	1
ChIP	Sequence-specific regulator	DIG1	Top 10%	5	1	1
ChIP	Sequence-specific regulator	DOT6	Top 10%	11	0	0
ChIP	Sequence-specific regulator	FHL1	Top 10%	6	0	4
ChIP	Sequence-specific regulator	FKH1	Top 10%	7	0	0
ChIP	Sequence-specific regulator	FKH2	Top 10%	8	1	1
ChIP	Sequence-specific regulator	FZF1	Top 10%	10	0	0
ChIP	Sequence-specific regulator	GAT1	Top 10%	6	0	1
ChIP	Sequence-specific regulator	GCN4	Top 10%	6	0	1
ChIP	Sequence-specific regulator	GCR1	Top 10%	14	1	1
ChIP	Sequence-specific regulator	GCR2	Top 10%	13	2	0
ChIP	Sequence-specific regulator	GLN3	Top 10%	8	0	0
ChIP	Sequence-specific regulator	GRF10(Pho2)	Top 10%	6	1	0
ChIP	Sequence-specific regulator	GTS1	Top 10%	6	0	1
ChIP	Sequence-specific regulator	HAA1	Top 10%	8	1	2
ChIP	Sequence-specific regulator	HAL9	Top 10%	17	1	0
ChIP	Sequence-specific regulator	HAP2	Top 10%	17	1	0
ChIP	Sequence-specific regulator	HAP3	Top 10%	13	0	0
ChIP	Sequence-specific regulator	HAP4	Top 10%	5	0	1
ChIP	Sequence-specific regulator	HAP5	Top 10%	12	1	0
ChIP	Sequence-specific regulator	HIR1	Top 10%	15	0	0
ChIP	Sequence-specific regulator	HIR2	Top 10%	9	0	0
ChIP	Sequence-specific regulator	HMS1	Top 10%	14	0	0

ChIP	Sequence-specific regulator	IME4	Top 10%	18	1	1
ChIP	Sequence-specific regulator	INO2	Top 10%	6	3	1
ChIP	Sequence-specific regulator	IXR1	Top 10%	5	1	1
ChIP	Sequence-specific regulator	LEU3	Top 10%	9	1	0
ChIP	Sequence-specific regulator	MAC1	Top 10%	9	0	0
ChIP	Sequence-specific regulator	MAL33	Top 10%	6	0	2
ChIP	Sequence-specific regulator	MATa1	Top 10%	15	0	0
ChIP	Sequence-specific regulator	MBP1	Top 10%	11	0	0
ChIP	Sequence-specific regulator	MCM1	Top 10%	7	1	0
ChIP	Sequence-specific regulator	MET31	Top 10%	11	0	0
ChIP	Sequence-specific regulator	MIG1	Top 10%	13	0	0
ChIP	Sequence-specific regulator	MOT3	Top 10%	7	0	1
ChIP	Sequence-specific regulator	MSN1	Top 10%	5	0	1
ChIP	Sequence-specific regulator	MSN2	Top 10%	7	0	0
ChIP	Sequence-specific regulator	MSS11	Top 10%	13	0	2
ChIP	Sequence-specific regulator	NDD1	Top 10%	6	0	0
ChIP	Sequence-specific regulator	PDR1	Top 10%	11	1	1
ChIP	Sequence-specific regulator	PHO4	Top 10%	5	0	0
ChIP	Sequence-specific regulator	RCS1	Top 10%	12	1	0
ChIP	Sequence-specific regulator	REB1	Top 10%	13	1	0
ChIP	Sequence-specific regulator	RFX1	Top 10%	17	1	0
ChIP	Sequence-specific regulator	RGT1	Top 10%	12	0	0
ChIP	Sequence-specific regulator	RLM1	Top 10%	7	0	0
ChIP	Sequence-specific regulator	RME1	Top 10%	6	0	0
ChIP	Sequence-specific regulator	ROX1	Top 10%	6	0	0
ChIP	Sequence-specific regulator	RPH1	Top 10%	6	0	0
ChIP	Sequence-specific regulator	RTG1	Top 10%	7	0	1
ChIP	Sequence-specific regulator	RTG3	Top 10%	5	1	1
ChIP	Sequence-specific regulator	RTS2	Top 10%	13	0	1
ChIP	Sequence-specific regulator	SFL1	Top 10%	7	0	1
ChIP	Sequence-specific regulator	SIG1	Top 10%	11	0	0
ChIP	Sequence-specific regulator	SIP4	Top 10%	8	0	1
ChIP	Sequence-specific regulator	SKO1	Top 10%	11	1	2
ChIP	Sequence-specific regulator	SMP1	Top 10%	6	0	0
ChIP	Sequence-specific regulator	SRD1	Top 10%	12	0	1
ChIP	Sequence-specific regulator	STB1	Top 10%	6	1	0
ChIP	Sequence-specific regulator	STE12	Top 10%	6	1	1
ChIP	Sequence-specific regulator	STP1	Top 10%	14	1	0
ChIP	Sequence-specific regulator	STP2	Top 10%	10	0	1
ChIP	Sequence-specific regulator	SWI5	Top 10%	6	1	0
ChIP	Sequence-specific regulator	SWI6	Top 10%	5	0	0
ChIP	Sequence-specific regulator	UGA3	Top 10%	6	0	0
ChIP	Sequence-specific regulator	USV1	Top 10%	5	0	0

ChIP	Sequence-specific regulator	YAP1	Top 10%	10	0	0
ChIP	Sequence-specific regulator	YAP3	Top 10%	5	2	1
ChIP	Sequence-specific regulator	YAP6	Top 10%	8	0	2
ChIP	Sequence-specific regulator	YAP7	Top 10%	5	0	1
ChIP	Sequence-specific regulator	YBR267W	Top 10%	6	0	1
ChIP	Sequence-specific regulator	YFL044C	Top 10%	15	0	0
ChIP	Sequence-specific regulator	YJL206C	Top 10%	10	1	0
ChIP	Sequence-specific regulator	ZAP1	Top 10%	14	0	0
Expression	nucleosome	*rpd3*Δ	Bot. 10%	0	23	3
Expression	Salt Stress	NaCl 30'	Bot. 10%	0	28	2
Expression	Oxidative Stress	Peroxide 20'	Bot.10%	1	22	0
Expression	SWI/SNF	*snf5*Δ	Bot. 10%	0	18	2
Expression	RAP1	*rap1* ts	Bot. 10%	0	19	2
Expression	Osmotic Stress	*rpd3*Δ (5min 0.4M NaCl)	Bot. 10%	1	14	3
Expression	nucleosome	H3Δ1-28	Bot. 10%	1	14	2
Group	Essential gene			2	11	5
DNA	Motif	Reb1		3	6	1
Expression	nucleosome	H4 dep. (6 hr)	Bot. 10%	3	12	56
Expression	RSC	*rsc30*Δ	Top 10%	6	1	57
Expression	Hos3	*hos3*Δ	Top 10%	4	6	40
Expression	SWR1	*swr1*Δ	Top 10%	1	0	22
ChIP	COMPASS	Set1	Top 10%	2	16	13
Expression	Mot1	*mot1-14*	Bot. 10%	0	6	22
Group	Rap1	Rap1 ChIP; RP		4	0	57

[a]The relationships analysis above lists the -Log_{10}(*P*-value) for overlap between membership in each group of genes from Figure 4A, and the top 10%, bottom 10%, or group/property membership from published microarray data sets. The published microarray datasets are arranged by category and described by the protein mutated or characteristic studied. The *P*-value was calculated using the Chi-test, and returns the probability that the overlap between two data sets occurs by chance. Thus, the most statistically significant relationships will have the largest -Log_{10}(*P*-value). Underrepresented relationships are colored in red.

Table S2. ChIP-chip false discovery rates (FDR[a]).

GTFs

	FDR (%)	Count
TBP	0.78%	1202
TFIIA (Toa2)	14.10%	189
TFIIB (Sua7)	0.00%	1180
TFIIE (Tfa1)	0.19%	1136
TFIIF (Tfg1)	0.09%	1253
TFIIH (Ssl1)	0.00%	1219

Co-activators

	FDR (%)	Count
TFIID (Taf1)	0.18%	1185
SAGA (Spt3)	0.62%	648

Pol II and mediator

	FDR (%)	Count
Pol II (Rpo21)	2.06%	1105
Mediator (Srb5)	2.52%	1141
Mediator (Nut1)	1.37%	1130
Mediator (Rgr1)	1.04%	1194

Chromatin Remodelers

	FDR (%)	Count
RSC (Rsc9)	0.79%	592
SWI/SNF (Swi3)	0.77%	599
ISW1a/b (Isw1)	0.61%	626
ISW1a (Ioc3)	5.29%	566
ISW1b (Ioc2)	2.27%	606
ISW2 (Isw2)	2.03%	594
INO80 (Ino80)	1.49%	576
SWR-C (Swr1)	0.19%	550

Sequence-specific regulators

	FDR (%)	Count
Rap1	0.60%	381
Ifh1	23.93%	87
Rfx1	6.35%	318
Xbp1	5.79%	336
Yap6	3.67%	304
Reb1	0.56%	307
Swi4	23.33%	96
Cin5	15.22%	189

[a]Please refer to the Methods section for details on FDR calculations.

Table S3: Genome-wide co-occupancy of sequence-specific regulators and chromatin remodelers.[a]

Chi-test -LOG$_{10}$(*P*-value) for pairwise co-occupancy overlap

Chromatin Remodelers		**Sequence-specific regulators**							
Complex		Rap1	Ifh1	Cin5	Swi4	Reb1	Rfx1	Xbp1	Yap6
ISW1a	Ioc3	1	2	1	0	3	91	170	57
ISW1b	Ioc2	1	1	1	0	3	75	117	45
ISW2	Isw2	0	2	1	0	4	41	57	31
SWI/SNF	Swi3	3	0	0	8	1	1	0	0
RSC	Rsc9	0	0	1	0	7	74	98	47
INO80	Ino80	3	0	2	1	11	47	45	35
SWR-C	Swr1	2	1	1	1	21	50	94	50

[a] The Excel Chi-test function was used to determine the statistical significance of promoter co-occupancy for the pairwise combinations between sequence-specific regulators and chromatin remodelers.

Table S4: Genome-wide spatial linkage of binding locations for sequence-specific regulators and chromatin remodelers.[a]

Standard deviation for pairwise distance between binding-sites

Chromatin Remodelers		**Sequence-specific regulators**							
Complex		Rap1	Ifh1	Cin5	Swi4	Reb1	Rfx1	Xbp1	Yap6
ISW1a	Ioc3	63	30	56	38	44	24	18	29
ISW1b	Ioc2	62	32	55	53	55	31	20	33
ISW2	Isw2	59	28	48	28	45	30	23	35
SWI/SNF	Swi3	53	49	48	19	53	47	44	55
RSC	Rsc9	56	32	54	24	31	24	23	32
INO80	Ino80	64	36	59	30	51	31	29	41
SWR-C	Swr1	54	60	51	35	37	25	21	33

[a]The distance standard deviation for the binding-sites for co-occupied promoters in each pairwise combination between sequence-specific regulators and chromatin remodelers was determined to assess location-linkage.

Table S5. Processed microarray data: Occupancy levels in YPD at 25°C.
•Shown below is small sample of data contained in Table S5.
•Also included are the genome-wide occupancy levels for 28 transcription factors determined using custom low-density tiling arrays. See excel file for complete data.
•The genome-wide occupancy levels for Reb1, TBP, Sua7, Swr1, Rsc9, Rpo21, and Rpb3 determined using high-density Affymetrix tiling arrays are available as wig files online at www.genome.org.
•The raw data for low-resolution arrays (i.e. gpr files) and high-resolution Affymetrix arrays (i.e. cel files) are available at ArrayExpress (http://www.ebi.ac.uk/arrayexpress/) under accession number A-MEXP-1161.

Type			ChIP TFIID/SAGA	ChIP TFIID/SAGA	ChIP
Type					TFIID/ SAGA
IP target			**TBP**	**TBP**	**TBP**
Reference			Null	Null	Null
Strain/Ab			BY4741	BY4741	BY4741
Growth Conditions			YPD @ 25C to A600=0.8-1	YPD @ 25C to A600=0.8-1	YPD @ 25C to A600=0.8-1
Data subset			AB	AB	AB
Facility and Reference			Venters	Venters	Venters
Platform			spotted	spotted	spotted
Gene_ID	**Common**	**Orientation**	**25C TSS**	**25C UAS1**	**25C ORF**
YAL001C	TFC3	T-H	1.29		0.12
YAL002W	VPS8	T-H	0.63	1.17	-0.51
YAL003W	EFB1	H-H			1.39
YAL005C	SSA1	H-H			0.37
YAL007C	ERP2	T-H	1.35	0.17	-0.37
YAL008W	FUN14	T-H	0.61	0.39	-0.27
YAL009W	SPO7	H-H	0.57	0.00	-0.34
YAL010C	MDM10	H-H		-0.78	-1.06
YAL011W	SWC1	T-H	-0.02	0.31	-0.03
YAL012W	CYS3	T-H	2.24	0.79	0.29
YAL013W	DEP1	H-H	1.51	0.24	0.50
YAL014C	SYN8	H-H	-0.27	-0.42	0.62
YAL015C	NTG1	T-H		-0.39	0.24
YAL016C-B				-0.46	
YAL016W	TPD3	T-H	1.11	1.49	0.50
YAL017W	PSK1	H-H	-0.51	0.89	
YAL018C		H-H	-0.98	0.78	

YAL019W	FUN30	H-H	-0.13	0.63

Table S6. Genome-wide binding-site locations relative to the TSS.

- Shown below is small sample of data contained in Table S6.
- Included in Table S6 are the interpolated binding locations for 28 transcription factors determined using custom low-density tiling arrays. Also included are the binding locations for Reb1, TBP, Sua7, Swr1, Rsc9, Rpo21, and Rpb3 determined using high-density Affymetrix tiling arrays.
- See excel file for complete data.

Type			ChIP	ChIP
Complex			TFIID/SAGA	TFIIB
IP target			**TBP**	**Sua7**
Reference			Null	Null
Strain/Ab			BY4741	Sua7-TAP
Growth Conditions			YPD @ 25C to A600=0.8-1, 25C	YPD @ 25C to A600=0.8-1, 25C
Data subset			AB	AB
Facility and Reference			Venters	Venters
Data transformation				
Platform			spotted	spotted
Median (relative to TSS)			-73	-56
Gene_ID	**Common**	**Orientation**	**25C Frac Occ**	**25C Frac Occ**
YAL001C	TFC3	T-H		
YAL002W	VPS8	T-H		
YAL003W	EFB1	H-H		
YAL005C	SSA1	H-H		
YAL007C	ERP2	T-H	-19	29
YAL008W	FUN14	T-H		
YAL009W	SPO7	H-H		
YAL010C	MDM10	H-H		
YAL011W	SWC1	T-H		
YAL012W	CYS3	T-H	-43	19
YAL013W	DEP1	H-H	-49	-34
YAL014C	SYN8	H-H		
YAL015C	NTG1	T-H		
YAL016C-B				
YAL016W	TPD3	T-H		
YAL017W	PSK1	H-H		
YAL018C		H-H		
YAL019W	FUN30	H-H		
YAL020C	ATS1	H-H		
YAL021C	CCR4	T-H		-60
YAL022C	FUN26	T-H		
YAL023C	PMT2	T-H	-23	9
YAL024C	LTE1	T-H		

References

Albert, I., T.N. Mavrich, L.P. Tomsho, J. Qi, S.J. Zanton, S.C. Schuster, and B.F. Pugh. 2007. Translational and rotational settings of H2A.Z nucleosomes across the Saccharomyces cerevisiae genome. *Nature* **446:** 572-576.

Bailey, T.L., N. Williams, C. Misleh, and W.W. Li. 2006. MEME: discovering and analyzing DNA and protein sequence motifs. *Nucleic Acids Res* **34:** W369-373.

Basehoar, A.D., S.J. Zanton, and B.F. Pugh. 2004. Identification and distinct regulation of yeast TATA box-containing genes. *Cell* **116:** 699-709.

David, L., W. Huber, M. Granovskaia, J. Toedling, C.J. Palm, L. Bofkin, T. Jones, R.W. Davis, and L.M. Steinmetz. 2006. A high-resolution map of transcription in the yeast genome. *Proc. Natl. Acad. Sci. USA* **103:** 5320-5325.

Eisen, M.B., P.T. Spellman, P.O. Brown, and D. Botstein. 1998. Cluster analysis and display of genome-wide expression patterns. *Proc Natl Acad Sci U S A* **95:** 14863-14868.

Harbison, C.T., D.B. Gordon, T.I. Lee, N.J. Rinaldi, K.D. Macisaac, T.W. Danford, N.M. Hannett, J.B. Tagne, D.B. Reynolds, J. Yoo et al. 2004. Transcriptional regulatory code of a eukaryotic genome. *Nature* **431:** 99-104.

Johnson, W.E., W. Li, C.A. Meyer, R. Gottardo, J.S. Carroll, M. Brown, and X.S. Liu. 2006. Model-based analysis of tiling-arrays for ChIP-chip. *Proc Natl Acad Sci U S A* **103:** 12457-12462.

Perocchi, F., Z. Xu, S. Clauder-Munster, and L.M. Steinmetz. 2007. Antisense artifacts in transcriptome microarray experiments are resolved by actinomycin D. *Nucleic Acids Res* **35:** e128.

Whitehouse, I., O.J. Rando, J. Delrow, and T. Tsukiyama. 2007. Chromatin remodelling at promoters suppresses antisense transcription. *Nature* **450:** 1031-1035.